

CFA/VISHNO 2016

Modélisation et simulation d'ondes acoustiques dans des milieux poreux périodiques fortement hétérogènesV.H. Nguyen^a, E. Rohan^b et S. Naili^a^aUniversité Paris-Est, MSME UMR 8208 CNRS, 61, Avenue du Général de Gaulle,
94010 Créteil, France^bUniversity of West Bohemia, European Centre of Excellence, NTIS, Faculty of Applied
Sciences, Univerzitní 22, 30614 Pilsen, République tchèque
vu-hieu.nguyen@u-pec.fr

LE MANS

Acoustical properties of heterogeneous and saturated rigid porous media with high permeability contrast is studied. At the mesoscopic scale, the movement of fluid is described by using the generalized Darcy's law. A two-scale homogenization method is employed to obtain the wave propagation equations at the macroscopic scale. By introducing a scale separation for high contrast permeability, a new quantity representing the dynamic compressibility is appeared in the macroscopic wave equations. The variational equations of local problems are presented for determining effective acoustic properties at the macroscale. The proposed method is validated by considering a problem of plane harmonic wave propagation in a halfspace. Solutions obtained by using the proposed homogenization method are compared with the finite element solutions computed by using a model with real mesoscopic geometry. The validity domain of high permeability contrast model is also discussed.

1 Introduction

Many natural/artificial porous materials exhibit the presence of heterogeneity at scales much larger than microstructure scales, but much smaller than the wavelengths. In a such porous medium with heterogeneity at the meso-scale, pore fluids in regions of dissimilar properties respond differently with changes in their fluid pressures. It significantly affects the velocity dispersion and attenuation, referred to as mesoscopic losses due to wave-induced flows [10]. Basically, continuum porous model with spatially varying coefficients may be used for simulating the wave propagation in a heterogeneous porous media. However, the simulation may be very costly, especially when the domain of interest is much larger than the heterogeneity's size. For media with periodically distributed inhomogeneities, macroscopic effective media can be derived from the continuum equations established at mesoscale. Effective material parameters have been derived by using volume-averaging technique for acoustic problem of porous media which consist of two linear isotropic porous constituents [1] and Pride and Berryman [8, 9]. However, situations of very high heterogeneity of permeability have not been addressed in previous works.

This note reports the essential procedure for determining the dispersion of acoustic waves at the macroscopic scale of high permeability contrast (HPC) porous media. More details can be found in [5].

2 Model and equations

2.1 Acoustic equations in rigid porous media

Let us consider a periodic rigid-skeleton porous medium occupying a domain Ω under time-harmonic excitation (the time dependence $e^{i\omega t}$, where $\omega = 2\pi f$ is the angular frequency, f is the frequency, and $i = \sqrt{-1}$). The porous medium with porosity ϕ_0 is saturated by a compressible and viscous fluid of density ρ^f and dynamic viscosity η . Following [2], the governing equations of wave propagation problem in Ω is given by:

$$\nabla_x \cdot \mathbf{w} + \frac{i\omega}{\mu} p = 0 \quad \text{in } \Omega, \quad (1)$$

$$\eta [\mathbf{k}(\omega)]^{-1} \mathbf{w} + \nabla_x p = \mathbf{0}, \quad \text{in } \Omega, \quad (2)$$

where $\mathbf{w}(\mathbf{x}, \omega)$ and $p(\mathbf{x}, \omega)$ are respectively the fluid's effective velocity and the interstitial fluid pressure; μ is the Biot modulus: $\mu = \phi_0^{-1} k^f$ with k^f the fluid's bulk modulus of the fluid; $\mathbf{k}(\omega)$ is the dynamic permeability tensor which contains the inertial drag and viscous effects due to the movement of interstitial fluid [6]. For an orthotropic

medium, and the complex-valued second-order tensor $\mathbf{k}(\omega)$ is diagonal and may be expressed by: $\mathbf{k} = \text{diag}(k_i)$ for $i = 1, \dots, 3$. For this study, we use Johnson-Koplik-Dashen (JKD) model [4] for which the component i of the diagonal tensor $\eta [\mathbf{k}(\omega)]^{-1}$ may be expressed by:

$$\frac{\eta}{k_i} = i\omega \frac{\rho^f a_i^\infty}{\phi_0} + \frac{\eta F_i^{\text{corr}}(\omega)}{k_{0i}}, \quad (3)$$

where a_i^∞ and k_{0i} are respectively the tortuosity and the intrinsic permeability in the direction i ; F_i^{corr} is a correction factor [4]:

$$F_i^{\text{corr}}(\omega) = \sqrt{1 + \frac{4i(a_i^\infty)^2 k_{0i}^2 \rho^f \omega}{\eta \Lambda_i^2 \phi_0^2}}, \quad (4)$$

where Λ_i is a geometrical parameter for which $2/\Lambda_i$ is the ratio between the surface and the volume of the pores. Noting that $F_i^{\text{corr}}(\omega)$ is complex, one may separate the viscous term from the inertia term in Eq. (2) by rewriting η/k_i (see Eq. (3)) in terms of real parameters ρ_i and K_i introduced by $\omega \rho_i = \Im(\eta/k_i)$ and $\eta/K_i = \Re(\eta/k_i)$, so that:

$$\eta [\mathbf{k}(\omega)]^{-1} = [\boldsymbol{\kappa}(\omega)]^{-1} = (i\omega \boldsymbol{\rho} + [\mathbf{K}]^{-1}). \quad (5)$$

where $\boldsymbol{\rho}$ and \mathbf{K} are diagonal real-valued tensors.

2.2 Periodic porous medium with high permeability contrast (HPC)

We assume that the porous medium in consider has a periodic and high-contrast permeability. A dimensionless scale parameter ε is introduced presenting the ratio between the characteristic size of the heterogeneity at the mesoscopic scale (characteristic length ℓ) and the wavelength which is comparable with a macroscopic size L , thus, $\varepsilon = \ell/L$. For a given ε , we may introduce the following split: $\Omega = \Omega_m^\varepsilon \cup \Omega_c^\varepsilon$ where Ω_m^ε is the subdomain with a low-permeability and Ω_c^ε is the subdomain with a high-permeability ($\Omega_m^\varepsilon \cap \Omega_c^\varepsilon = \emptyset$) (see Fig. 1). Since we consider a periodic media, all material parameters are assumed to be periodic with respect to the spatial position.

In each REV, the material parameters are assumed to take the form (see Rohan et al. [12]):

$$\begin{aligned} \boldsymbol{\rho}(\mathbf{y}) &= \chi_c(\mathbf{y}) \boldsymbol{\rho}_c + \chi_m(\mathbf{y}) \boldsymbol{\rho}_m, \\ \boldsymbol{\mu}(\mathbf{y}) &= \chi_c(\mathbf{y}) \boldsymbol{\mu}_c + \chi_m(\mathbf{y}) \boldsymbol{\mu}_m, \end{aligned} \quad (6)$$

$$[\mathbf{K}(\mathbf{y})]^{-1} = \chi_c(\mathbf{y}) \mathfrak{R}([\mathbf{K}_c]^{-1}) + \varepsilon^{-2} \chi_m(\mathbf{y}) [\widehat{\mathbf{K}}_m]^{-1},$$

where $\chi_c(\mathbf{y}) = 1$, $\chi_m(\mathbf{y}) = 0$ for $\mathbf{y} \in Y_c$, and $\chi_c(\mathbf{y}) = 0$, $\chi_m(\mathbf{y}) = 1$ for $\mathbf{y} \in Y_m$.

The convergence results, as obtained rigorously in [11] using the periodic unfolding method of homogenization,

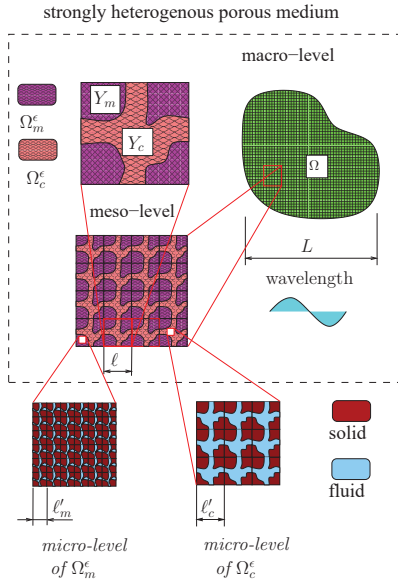


Figure 1: Description d'un milieu poreux périodique avec un contraste élevé de perméabilité

yield the two-scale asymptotic expansions in ε of $p^\varepsilon(\mathbf{x}, \omega)$ and $\mathbf{w}^\varepsilon(\mathbf{x}, \omega)$ which take the following form:

$$\begin{aligned} p^\varepsilon(\mathbf{x}) &= p^0(\mathbf{x}) + \varepsilon \chi_c(\mathbf{y}) P^1(\mathbf{x}, \mathbf{y}) + \chi_m(\mathbf{y}) \hat{p}(\mathbf{x}, \mathbf{y}), \\ \mathbf{w}^\varepsilon(\mathbf{x}) &= \chi_c(\mathbf{y}) \mathbf{W}(\mathbf{x}, \mathbf{y}) + \varepsilon \chi_m(\mathbf{y}) \hat{\mathbf{w}}(\mathbf{x}, \mathbf{y}), \end{aligned} \quad (7)$$

where P^1 , \hat{p} , \mathbf{W} and $\hat{\mathbf{w}}$ are Y -periodic functions. These truncated expansions reveal completely different asymptotic behaviour of the pressure and velocity fields in Y_c and Y_m .

2.3 Homogenized HPC model

2.3.1 Local problem at mesoscopic scale

Local problems in Y_c and Y_m govern the characteristic responses (see [11] for details). We shall use the space $\mathcal{P}(Y_d)$ formed by sufficiently differentiable Y -periodic functions restricted to Y_d , $d = m, c$.

Local problem in Y_c Functions P^1 and \mathbf{W} involved in (7) are expressed by the following relations [11]:

$$P^1 = i\omega \pi^k (\partial_k^x p^0 - f_k), \quad \mathbf{W} = i\omega \psi^k (\partial_k^x p^0 - f_k), \quad (8)$$

where π^k and ψ^k are the characteristic Y -periodic responses for a fixed frequency ω .

The characteristic response π^k ($k = 1, \dots, 3$) is a Y -periodic function defined in subdomain Y_c ; for a given ω , function π^k satisfies the following equations:

$$\nabla_{\mathbf{y}} \cdot \left\{ \boldsymbol{\kappa}_c \nabla_{\mathbf{y}} \left(\pi^k + \frac{1}{i\omega} y_k \right) \right\} = 0, \quad \forall \mathbf{y} \in Y_c, \quad (9)$$

$$\mathbf{n} \cdot \boldsymbol{\kappa}_c \nabla_{\mathbf{y}} \left(\pi^k + \frac{1}{i\omega} y_k \right) = 0, \quad \forall \mathbf{y} \in \partial Y_c \setminus \partial Y, \quad (10)$$

where $\boldsymbol{\kappa}_c(\omega) = (i\omega \rho_c + [\mathbf{K}_c]^{-1})^{-1}$; $\nabla_{\mathbf{y}}$ and $\nabla_{\mathbf{y}} \cdot$ denote the gradient and divergence operators with respect to \mathbf{y} , respectively. The flux vector ψ^k may be calculated in terms of π^k :

$$\psi^k = -\boldsymbol{\kappa}_c(\omega) \nabla_{\mathbf{y}} \left(\pi^k + \frac{1}{i\omega} y_k \right). \quad (11)$$

The problem (9)-(10) can be solved using the weak formulation: Find $\pi^k \in \mathcal{P}(Y_c)$, such that:

$$\int_{Y_c} \nabla_{\mathbf{y}}(\delta\pi) \cdot \boldsymbol{\kappa}_c \nabla_{\mathbf{y}} \left(\pi^k + \frac{1}{i\omega} y_k \right) dV_{\mathbf{y}} = 0, \quad (12)$$

for $\forall \delta\pi \in \mathcal{P}(Y_c)$.

Local problem in Y_m Functions \hat{p} and $\hat{\mathbf{w}}$ are expressed by the following relations (see Rohan [11]):

$$\hat{p} = -\omega^2 \hat{\pi} p^0, \quad \hat{\mathbf{w}} = -\omega^2 \hat{\chi} p^0, \quad (13)$$

where $\hat{\pi}$ and $\hat{\chi}$ are the characteristic Y -periodic responses for ω fixed. Let us note that $\hat{p}(\mathbf{x}, \mathbf{y}) = 0$ in Y_c and have zero trace on the interface $Y_m \cap Y_c$. The characteristic response $\hat{\pi}$ is a Y -periodic scalar function defined in the subdomain Y_m ; for a given ω , $\hat{\pi}$ satisfies the following boundary-valued problem:

$$-\nabla_{\mathbf{y}} \cdot (\widehat{\mathbf{K}}_m \nabla_{\mathbf{y}} \hat{\pi}) + \frac{i\omega}{\mu_m} \hat{\pi} = -\frac{1}{i\omega \mu_m}, \quad \forall \mathbf{y} \in Y_m, \quad (14)$$

$$\hat{\pi} = 0, \quad \forall \mathbf{y} \in \partial Y_m \setminus \partial Y. \quad (15)$$

The vector function $\hat{\chi}$ is given by:

$$\hat{\chi} = \widehat{\mathbf{K}}_m \nabla_{\mathbf{y}} \hat{\pi}. \quad (16)$$

The variational equations of the problem (14)-(15) read: Find a Y -periodic $\hat{\pi} \in \mathcal{P}_0(Y_m)$ such that:

$$\begin{aligned} \int_{Y_m} \nabla_{\mathbf{y}}(\delta\hat{\pi}) \cdot \widehat{\mathbf{K}}_m \nabla_{\mathbf{y}} \hat{\pi} dV_{\mathbf{y}} + \int_{Y_m} \delta\hat{\pi} \frac{i\omega}{\mu_m} \hat{\pi} dV_{\mathbf{y}} \\ = - \int_{Y_m} \frac{1}{i\omega \mu_m} \delta\hat{\pi} dV_{\mathbf{y}}, \end{aligned} \quad (17)$$

for $\forall \delta\hat{\pi} \in \mathcal{P}_0(Y_m)$, where $\mathcal{P}_0(Y_m) = \{q \in \mathcal{P}(Y_m) \mid q = 0 \text{ on } \partial Y_m \setminus \partial Y\}$.

It is worth noting that the local problem in Y_m can be formulated equivalently in the real-sized cell εY , *i.e.* solved in εY_m for the natural permeability $\mathbf{K}_m = \varepsilon^2 \widehat{\mathbf{K}}_m$, whereby the gradients are $\nabla_x = \varepsilon^{-1} \nabla_{\mathbf{y}}$.

2.3.2 Global macroscopic problem in Ω

The acoustic wave propagation in the homogenized HPC medium obeys the following equation:

$$i\omega \nabla \cdot \mathcal{K}^H \nabla p^H + \omega^2 (Q - \omega^2 \mathcal{N}) p^H = 0, \quad (18)$$

where p^H is the local amplitude of the time-harmonic wave for the HPC model. In this model, the quantities Q and \mathcal{N} designate respectively the effective static compressibility and the effective dynamic compressibility; the second-order tensor \mathcal{K}^H represents the effective dynamic permeability divided by fluid viscosity. These three effective material parameters depend on the characteristic mesoscopic responses π^k and $\hat{\pi}$:

$$\mathcal{K}_{kl}^H = -\omega^2 \int_{Y_c} \boldsymbol{\kappa}_c \nabla_{\mathbf{y}} \left(\pi^k + \frac{1}{i\omega} y_k \right) \cdot \nabla_{\mathbf{y}} \left(\pi^l + \frac{1}{i\omega} y_l \right) dV_{\mathbf{y}}. \quad (19)$$

$$Q = \int_Y \frac{1}{\mu} dV_{\mathbf{y}}, \quad (20)$$

$$\mathcal{N} = - \int_{Y_m} \left(i\omega \widehat{\mathbf{K}}_m \nabla_{\mathbf{y}} \hat{\pi} \cdot \nabla_{\mathbf{y}} \hat{\pi} - \omega^2 \frac{1}{\mu_m} \hat{\pi} \hat{\pi} \right) dV_{\mathbf{y}}. \quad (21)$$

One may notice that the form of macroscopic model (18) is analogous with the one obtained in [7] and [3] which has been developed for the case in which Y_c is not a porous medium but a fluid.

3 Numerical results

To illustrate the proposed method, the plane wave problem in a 2D periodic porous halfspace. Fig. 2 shows the domain Y of the REV at the mesoscale represented by the rectangle $L_1 \times L_2$. At the mesoscale, Ω_c consists of orthogonal connected channels. The widths of channels in two orthogonal directions are denoted by h_1 and h_2 , respectively. We introduce a parameter $\phi_0^c = |Y_c|/|Y|$ which represents the volume fraction of Ω_c over Ω .

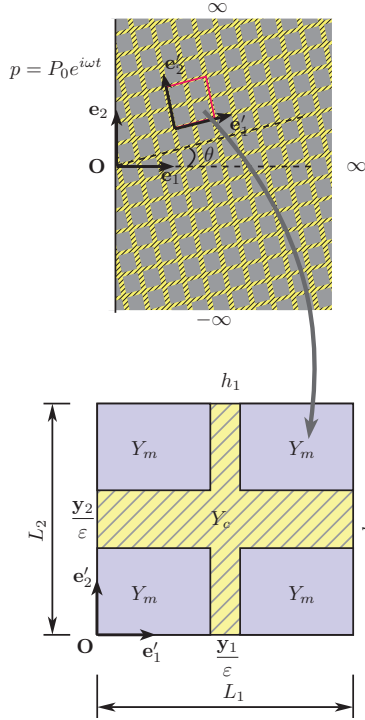


Figure 2: Halfspace with orthogonal Y_c channel REV.

For the simulation presented here, $L_1 = L_2 = 0.01$ m, $h_1 = 0.4L_1$ and $h_2 = 0.25L_2$. Both Ω_c and Ω_m are occupied by isotropic materials with the permeabilities $\kappa_0^m = 10^{-12}$ m²/(Pa.s) and $\kappa_0^c = 10^{-6}$ m²/(Pa.s), respectively. The bulk modulus and the dynamic viscosity of the fluid are given by $k^f = 2.25$ GPa and $\eta = 10^{-3}$ Pa.s⁻¹, respectively. Since the geometry is nonsymmetric (*i.e.* $h_1 \neq h_2$) at the mesoscale, the homogenized material is anisotropic at the macroscale. A time-harmonic pressure (with a constant amplitude P_0 and angular frequency ω) is applied at the surface $x_1 = 0$ to generate a plane wave in the \mathbf{e}_1 direction. The angle of incidence $\theta = \widehat{(\mathbf{e}'_1, \mathbf{e}_1)}$ defines the orientation of REV with respect to the wave propagation direction (see Fig. 2). In particular, we have chosen angle $\theta = \arctan(1/2)$, recalling its definition above. This specific choice is convenient to obtain a structure that have periodic boundary condition. The finite element element solution of the pressure field p is depicted in Fig. 3. One may note that the structural period with respect to the imposed wave direction (\mathbf{e}_1) is now $2L_1/\cos\theta \sim 0.022$ m.

Fig. 4 presents the validations for the solutions of the problem presented in Fig. 3 for the homogenized HPC model (the macroscopic response with and without correction terms) along two lines (C1): $x_2 = 0$ m (top) and (C2): $x_2 = 8 \times 10^{-3}$ m (bottom) (Fig. 3). It shows that the HPC model provides a very good approximation of the

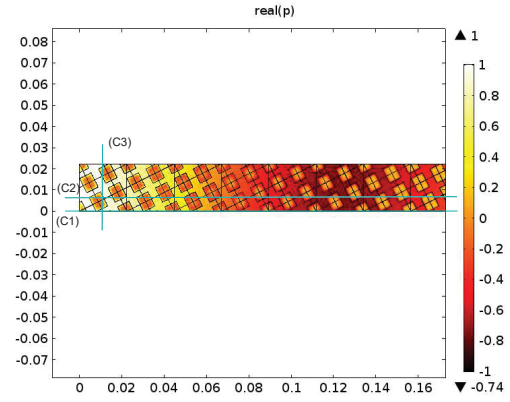


Figure 3: Finite element solution of pressure field $\text{Re}(p)$ in Pa ($\omega = 2.5 \times 10^4$ rad/s, $\tan\theta = 0.5$).

waveform at the macroscopic scale. Moreover, By using the correction p_H^{corr} , one may capture precisely the local responses at the mesoscale.

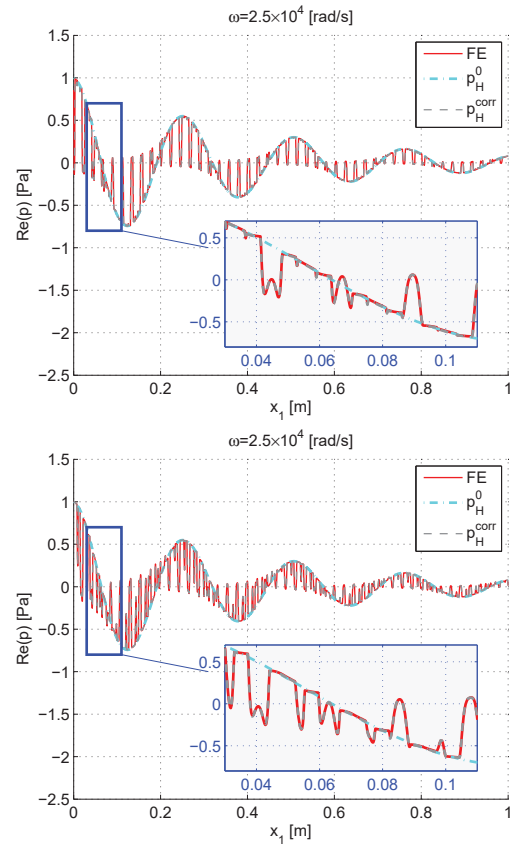


Figure 4: Comparison between the solutions of the HPC model and the reference FE solutions ($\tan\theta = 0$): pressure distributed along horizontal lines (C1): $x_2 = 0$ (top) and (C2): $x_2 = 0.008$ m (bottom) (see Fig. 3).

The macroscopic phase velocity and attenuation in a half-space with (with $\theta = 0$) is studied in Fig. 5. For comparison purposes, solutions obtained by using a model with low permeability contrast (LPC) is also presented. While for homogenized model the wave dispersion may be derived analytically, for the heterogeneous structure, it is computed numerically by using the FE solutions. One may notice that the macroscopic phase velocity and the

attenuation can be computed with a sufficient accuracy using one of the two homogenized models, *i.e* each of LPC and HPC models has its range of applicability. The expected critical contrast value, from which the HPC model would need to be employed in order to take into account the permeability scaling, may be given by the condition $\omega^2 N/Q = \bar{\mathcal{K}}_n/\mathcal{K}_n^L$ (more detail of this condition may be found in [5]). Hence, one suggest that for a given contrast level of permeability, one need to choose appropriate model for predicting the phase velocity and attenuation of the equivalent medium.

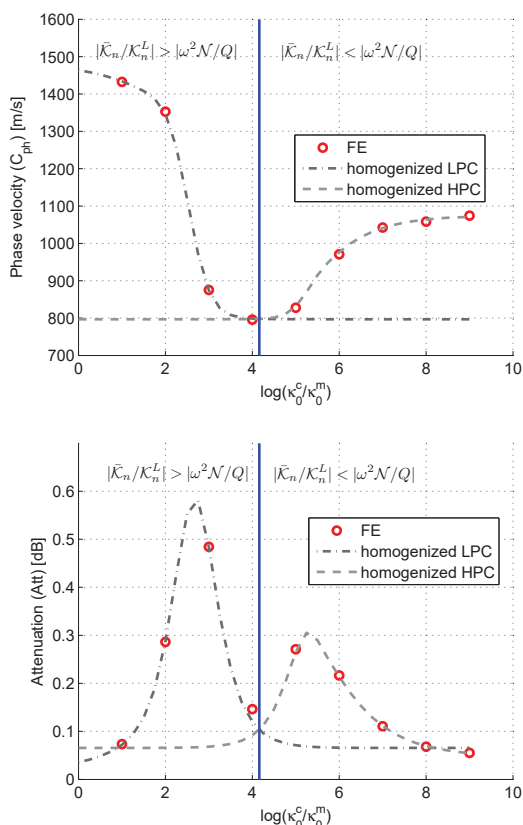


Figure 5: Phase velocities and attenuations computed using homogenized and original models ($\theta = 0$, $\omega = 2.5 \times 10^4$ rad/s).

4 Conclusion

Acoustic behaviors of a strongly heterogeneous porous medium can efficiently be predicted using the proposed two-scale homogenized HPC model [5, 11]. The scale separation of the permeability at the meso-scale lead to a new quantity (dynamic compressibility) in the macroscopic wave equation. The proposed procedure is useful for investigate the dynamic behavior of porous media with complex geometry of phases in REV at the mesoscale. The numerical results have shown that the local response at the mesoscopic level may be captured very well by using the homogenized model. An ongoing work is realized for studying dynamic behaviors of periodic poroelastic media with high contrasts on permeability/elasticity.

Acknowledgments

The research of the V.-H. Nguyen and S. Naili is supported by the CNRS-UPE project PEPS-2015-5. The research of the second author (E. Rohan) is supported by the Czech Scientific Foundation project GACR P101/12/2315.

References

- [1] J.B. Berryman and H.F. Wang. Elastic wave propagation and attenuation in a double-porosity dual-permeability medium. *Rock Mechanics and Mining Sciences*, 37:63–78, 2000.
- [2] M.A. Biot. Theory of propagation of elastic waves in a fluid-saturated porous solid. II. Higher-frequency range. *J. Acoust. Soc. Am.*, 28(2):179–191, 1956.
- [3] C. Boutin, P. Royer, and J.-L. Auriault. Acoustic absorption of porous surfacing with dual porosity. *Int. J. Solids and Structures*, 35:4709–4737, 1998.
- [4] D. Johnson, J. Koplik, and R. Dashen. Theory of dynamic permeability and tortuosity in fluid-saturated porous media. *J. Fluid Mech.*, 176:379–402, 1987.
- [5] Vu-Hieu Nguyen, Eduard Rohan, and Salah Naili. Multiscale simulation of acoustic waves in homogenized heterogeneous porous media with low and high permeability contrasts. *International Journal of Engineering Science*, 101:92 – 109, 2016.
- [6] A.N. Norris. On the viscodynamic operator in Biot’s equations of poroelasticity. *J. Wave-Material Interaction*, 1:365–380, 1986.
- [7] X. Olyny and C. Boutin. Acoustic wave propagation in double porosity media. *J. Acoust. Soc. Am.*, 114:73–89, 2003.
- [8] S.R. Pride and J.G. Berryman. Linear dynamics of double-porosity dual-permeability materials. I. Governing equations and acoustic attenuation. *Phys. Rev. E*, 68(036603):1–10, 2003.
- [9] S.R. Pride and J.G. Berryman. Linear dynamics of double-porosity dual-permeability materials. II. Fluid transport equations. *Phys. Rev. E*, 68(036604):1–10, 2003.
- [10] S.R. Pride, J.G. Berryman, and J.M. Harris. Seismic attenuation due to wave-induced flow. *J. Geophys. Res.*, 109(B01201), 2004.
- [11] E. Rohan. Homogenization of acoustic waves in strongly heterogeneous porous structures. *Wave Motion*, 50:1073–1089, 2013.
- [12] E. Rohan, S. Naili, R. Cimrman, and T. Lemaire. Multiscale modeling of a fluid saturated medium with double porosity: Relevance to the compact bone. *Jour. Mech. Phys. Solids*, 60:857–881, 2012.